

## Article

# Nonlinear Mixed Effect Model Used in a Simulation of the Impact of Climate Change on Height Growth of *Cyclobalanopsis glauca*

Huiliang Duan <sup>1</sup> and Gui Zhang <sup>2,\*</sup>

<sup>1</sup> College of Forestry, Central South University of Forestry and Technology, Changsha 412000, China; flduan@csuft.edu.cn

<sup>2</sup> College of Science, Central South University of Forestry and Technology, Changsha 412000, China

\* Correspondence: administrator@csuft.edu.cn; Tel.: +86-731-85623114

**Abstract:** Localized climate is sensitive to terrain, underlying surface material, building distribution, green coverage and CO<sub>2</sub> emissions. The Regional Climate Model (RegCM) was used to make a statistical detailed analysis of the climate change data in a specific study area to obtain fine-scale distribution of climatic elements data over time. The effects of climate change factors on height growth trends of a climate-sensitive tree species (*Cyclobalanopsis glauca*) were simulated based on historical climate base line data (1961–2010) and future climate change (2010–2100) predictions. *Cyclobalanopsis glauca* growth trends were simulated and analyzed by using a nonlinear mixed effect model (NLME). The results showed that under the RCP8.5 emissions scenario, the growth promotion effect on the height growth of *Cyclobalanopsis glauca* will be obvious. Under RCP4.5 and RCP2.6 emissions scenarios, although the inhibition intensity is not exactly the same, height growth will still be inhibited to a certain extent, which may lead to the gradual extinction of this species, affecting the composition of dominant tree species in the study area. The results indirectly reflect the impact of climate change on tree species diversity in the future.

**Keywords:** RegCM; downscaling; climate sensitive tree species; nonlinear mixed effect model; height growth of tree; tree species diversity



**Citation:** Duan, H.; Zhang, G. Nonlinear Mixed Effect Model Used in a Simulation of the Impact of Climate Change on Height Growth of *Cyclobalanopsis glauca*. *Forests* **2022**, *13*, 463. <https://doi.org/10.3390/f13030463>

Academic Editors: Alessio Collalti and Phillip G. Comeau

Received: 30 January 2022

Accepted: 14 March 2022

Published: 16 March 2022

**Publisher's Note:** MDPI stays neutral with regard to jurisdictional claims in published maps and institutional affiliations.



**Copyright:** © 2022 by the authors. Licensee MDPI, Basel, Switzerland. This article is an open access article distributed under the terms and conditions of the Creative Commons Attribution (CC BY) license (<https://creativecommons.org/licenses/by/4.0/>).

## 1. Introduction

The trend of climate warming is still continuing, and climate warming will lead to the extension and acceleration of the tree growth period. There is a general consensus that climate change will have various effects on forest ecosystems [1–3]. Due to many uncertain factors, it is difficult to establish a definitive model to simulate the impact of climate change on the growth of forest tree species, and to obtain reliable conclusions. The research on the impact of climate change on tree species diversity has, therefore, not received due attention. At present, more attention is paid to the impact of single climate factors on tree species diversity [4], and current research focuses on the radial growth of tree species and the impact of climate change on the phenological period [5], and it is rare to study the response of tree species diversity to climate change, especially on a fine scale.

The aim of this study was to estimate the potential change in vertical growth rates in trees as a result of climate change, through the application of a Nonlinear Mixed Effect Model (NLME) and Regional Climate Model (RegCM), combined to obtain a fine-scale model of the potential changes in tree species diversity due to the moderate interference of cause by human activities. In order to simulate growth trends of a climate sensitive tree species, where vertical growth is inhibited or promoted by climate change, the logistic basic growth model was combined with a mixed effect model, and an optimal growth model was selected. The tree vertical growth trend of *Cyclobalanopsis glauca* under various climate change scenarios was then simulated.

## 2. Study Area

Changes in tree species diversity are not only caused by climate but are also affected by human activities and other factors [6]. The continuous urbanization process is bound to reduce vegetation cover and change the underlying surface material [7,8], and will eventually lead to fundamental changes in the local climate, resulting in large changes in the regional climate. According to the forest vegetation type and the degree of interference by human activities, three typical sample plots were randomly selected in the study area by using the typical sample plot method [9]. In this study, the scale of economic development and human activities interference, and the level of economic development, in Wangcheng County, Changsha City, Hunan Province is moderate, and the effect on the environment is representative. In the research area, the main soil types included paddy soil, as well as yellow soil, red soil, brown soil and purple soil, etc. [10]. The three sample plots had been disturbed by human activities to varying degrees, the plots are characterized by the same physiographic conditions (slope < 15% and mean elevation about 150 m), and the straight line distance between plots is about 20 km. The geographical locations are shown in Figure 1, and the stars mark the positions of three plots. The degree of human activities, soil type and dominant tree species in each plot are briefly described as follows:

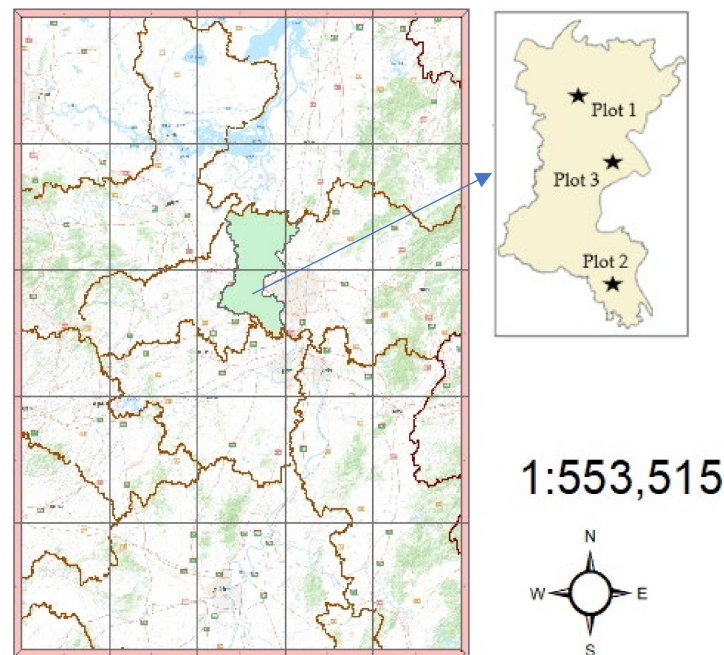


**Figure 1.** Location of the Wangcheng study areas within Hunan Province (scale 1:553,515).

**Plot 1:** Red soil with a heavy soil viscosity and less organic matter with less human interference, comprising mainly natural secondary forest: dominant tree species include *Pinus massoniana* Lamb, Taxodiaceae, *Castanopsis fargesii* Franch, *Cyclobalanopsis glauca*, *Castanopsis fabri*.

**Plot 2:** Yellow soil with a thick humus layer and a strongly acidic topsoil, with more human disturbance, comprising mainly natural secondary forest: dominant tree species include *Pinus massoniana* Lamb, Taxodiaceae, *Cyclobalanopsis glauca*, *Liquidambar formosana* Hance, *Castanopsis fabri*.

**Plot 3:** Brown soil with a texture of clay and sandy soil with low organic matter content, with the greatest interference from human activities, comprising mainly local tree species and artificially introduced alien tree species: dominant tree species include Taxodiaceae, *Cyclobalanopsis glauca*, Bambusoideae, *Liquidambar formosana* Hance, *Davidia involucrata* Baill, *Eucommia ulmoides*.

*Cyclobalanopsis glauca*, also known as ring-cupped oak, or Japanese blue oak in the west, is widely distributed from the eastern Himalayas to southern Japan, and from China's

Qingling-Huai River to the Malay Archipelago. It is an important tree species that is a major constituent of East Asian tropical and subtropical evergreen broad-leaved forests and, due to its sensitivity to climate change, it has important ecological functions [11]. In this paper, *Cyclobalanopsis glauca* was chosen as the indicative tree species of climate change.

The selected sample plots are in the stable stage of community succession. The plots are 20 m<sup>2</sup>, and the composition of tree species in the sample plots is relatively stable. Six *Cyclobalanopsis glauca*, in the 33–54 age-range with good growth and no diseases and pests, were randomly selected in each sample plot and cut down in July 2016. The trunks were analyzed using the cross-sectional method [12], and DBH, tree height and crown width were measured. DBH was used to classify age, with DBH < 3 cm classified as the first age-range with each subsequent age-range covering 4 cm. In order to reduce the complexity of the analysis, the competition between trees was not considered, and a total of 18 groups of single tree growth data were obtained.

### 3. Climate Change Model

#### 3.1. Future Climate Change Scenarios

Using a climate change model to accurately predict present and past climatic change can verify its validity for predicting future climate change, especially climate change caused by the increase in greenhouse gasses. In recent years, climate change simulation models have been developed to become more comprehensive and reliable, and can now be used to study the role of climate change at different time scales, predict the possible impact of human activities on climate, and provide large-scale climate transformation forecasts. The Sixth Coupled Model Intercomparison Project (CMIP6) comprises 33 institutions all over the world and consists of 112 climate models [13]. CMIP6 has become the richest source of numerical model designs and holds the largest amount of simulation data since the implementation of the Coupled Model Intercomparison Project [14]. These data are designed to support global climate research over the next 5–10 years [13]. Extreme high emission scenario Representative Concentration Pathway 8.5 (RCP8.5), moderate emission scenario RCP4.5 (RCP4.5) and low emission scenario RCP2.6 (RCP2.6) were used as the three climate change scenarios in this paper. To date, a large number of research achievements have been made in the prediction of climate change in the future, and although there are differences in the predicted results of future climate change under different scenarios by different climate change models, the predictions for simulations of future climate change are generally consistent: that the global temperature will continue to increase, and precipitation will increase regionally [15], which are affected by scale, terrain and other factors [16], and there will also be obvious regional differences [17].

In the present study, the study area is located in the middle of Hunan Province due to the differences of terrain, underlying surface material, building layout and green coverage; however, the climate characteristics in the near ground atmosphere are different from the general regional climate. One of the important objectives of developing regional, or local, climate models is to better reflect the characteristics of regional climate change by considering higher resolution features than those employed in global climate models [16]. The effects of climate change on vegetation distribution on a more regional scale results in greater detail than when global or continental scale vegetation models are used. It is therefore necessary to use the downscaling method for data resolution, so as to obtain accurate climate change data, in order to better combine with global climate change. This also allows for more accurate tree species diversity and distribution information to be taken into account in the climate change scenario. In addition to details concerning the specific simulated area, the selection of the resolution of the simulated network will also significantly affect the simulation results [18]. Due to the scope of the study area and the limited resolution of RegCM, a grid spacing of 5 km × 5 km was selected.

RegCM is a three-dimensional numerical climate model, which can be applied to any region of the world and for a wide range of studies, from process studies to paleoclimate and future climate simulations. It consists of four modules, including: main program,

parameter setting, initial side boundary of climate data and the post-processing module. The downscaling process of climate data was divided into three stages: initial conditions preparation, downscaling simulation and post-processing. The main program was the control program of mode operation, including the simulation of period, simulation scope and the definition of necessary parameters required for downscaling. In this study, 1961–2100 was selected as the period of climate changes simulation. This is consistent with CMIP6 data [19], and also maintains the age range (33–54 years) consistent with the range of growth data for *Cyclobalanopsis glauca* trees within the sample plots. The climate data from 1961 to 2010 were used as the historical base line, and climate data from 2010 to 2100 were used to calculate further climate change.

Downscaling is an important approach to obtaining fine-scale weather and climate information, and this was achieved by integrating RegCM with the initial and lateral boundary conditions from a general circulation model (GCM), an approach that has been widely reported [20,21]. Downscaling simulations are, however, often degraded by biases due to the large-scale data. In order to avoid the uncertainty of boundary values on the accuracy of our climate model and to reduce the influence of the selected marginal conditions, a larger simulation representing a greater geographical area was needed. The granularity of grid, including horizontal grids, and the geographical extent of the simulation divided by the grid distance were all defined with this in mind. In addition, an area three times the scope of the study area was selected, with a horizontal resolution of 5 km × 5 km to improve the accuracy of the climate model and to simulate as much detail as possible. The horizontal grids were set to 64 × 34 and vertical grids set to 18 (fixed value) [22]. Initial conditions were also defined, including terrain parameters, global terrain and land-type data point resolution ntypes set as 5 km (ntypes = 5), and similar ntypec, for sub grids ntypes\_set as 2 km (ntypes\_s = 2); initial and boundary conditions, SST data type set as OI\_W (sststyp = "oi\_wk"), global reanalysis data types set as NNRP1 (dattyp = "NNRP1"); center longitude and latitude of the simulated area as (114.5° E, 28° N); historical climate data simulation start and end date set as (globidata1 = 1961010100, globidate2 = 2010010100), and further climate data simulation start time and end date set as (idate1 = 2010010100, idate2 = 2100010100); radiation model time step set as 30 (radfrq = 30), atmospheric model time step set as 30 (dt = 30) and boundary condition frequency set as 6 (ibdyfrq = 6); map projection selected model defaults as lambert projection. Post processing comprised the adaptive conversion processing of the output results of climate models.

The results of climate change prediction in previous studies show that the model has good simulation ability for regional climate [23–25] and can give a detailed description of the temporal and spatial distribution of climate change characteristics in a specific study area. Due to a large number of climate variables output by the regional climate model, a principal component analysis was undertaken for these factors to reduce the quantity of data involved in the calculation, as described in Section 4.1.

### 3.2. Distribution of Climatic Elements

The output of the RegCM model and climate observation dataset CRU (climatic research unit) were spatially interpolated. The CRU TS is one of the most widely used observed climate datasets and is produced by the UK's NCAS (National Centre for Atmospheric Science) at the University of East Anglia's Climatic Research Unit [26]. In order to ensure the accuracy of meteorological element interpolation results and to better reflect the topographic factors, ASTER Global Digital Elevation Model was employed. Aster GDEM is a global digital elevation data product jointly released by NASA. The horizontal accuracy of the data is 1" (about 30 m, confidence 95%), and the elevation accuracy is 20 M (confidence 95%) [27]. The Digital Elevation Model (DEM) was used as a covariate in the interpolation process. According to the climate model, the monthly average temperature in the study area was 13.1 °C from 1961 to 2010; the average temperature of the hottest month, July, was 27 °C, distribution shown in Figure 2; the average temperature of the coldest month, January, was 2 °C, shown in Figure 3; and the average annual precipitation was 740 mm,

shown in Figure 4. In order to consider scale issues and to show as much detail as possible, the distribution maps of climatic elements shown as Figures 2–4 are a representative part of the study area.

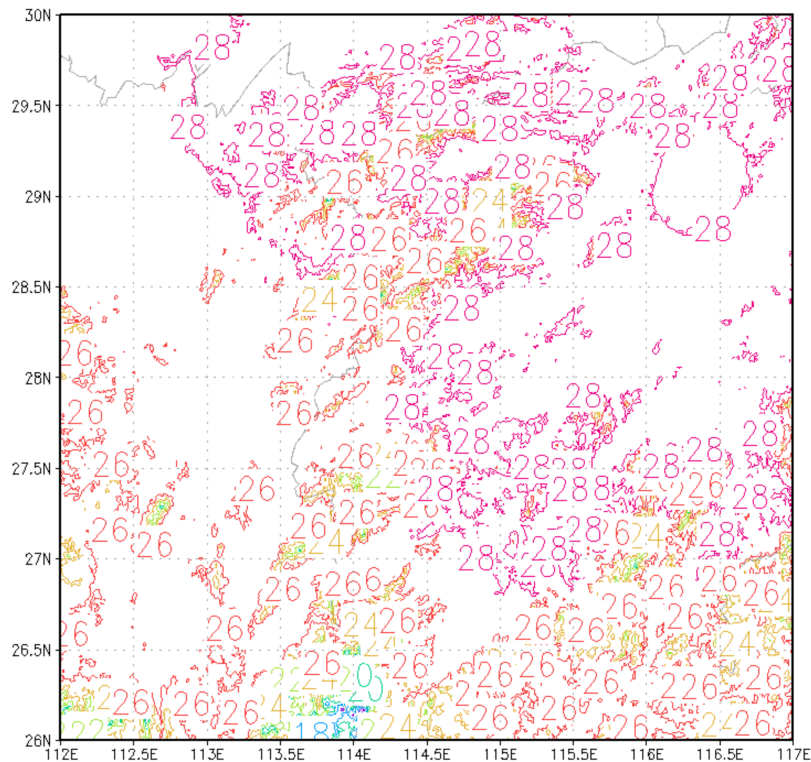


Figure 2. Average temperature (°C) of the hottest month, July, from 1961 to 2010.

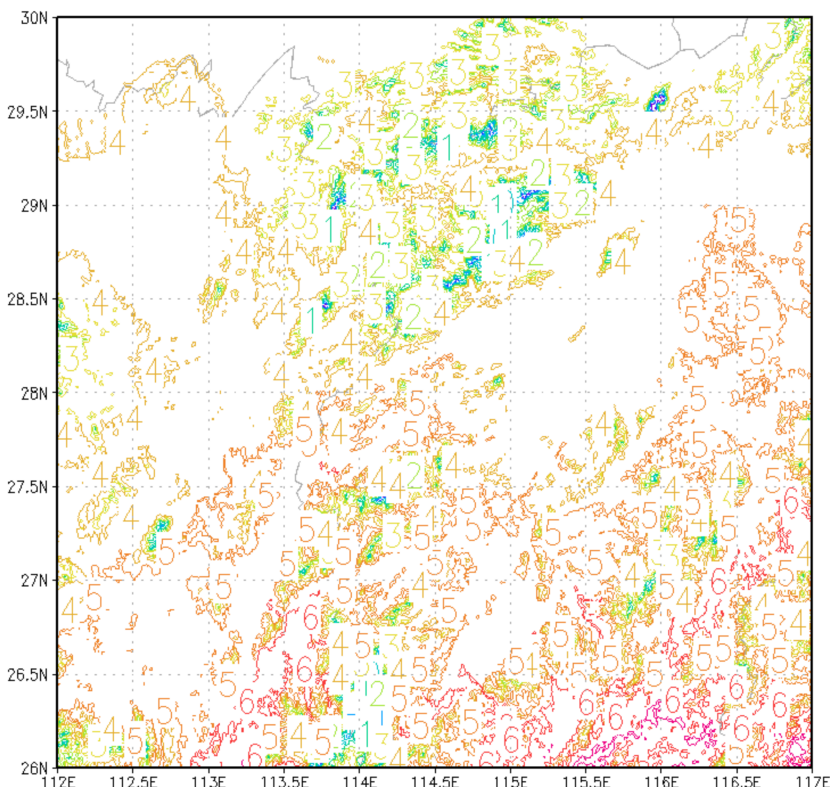
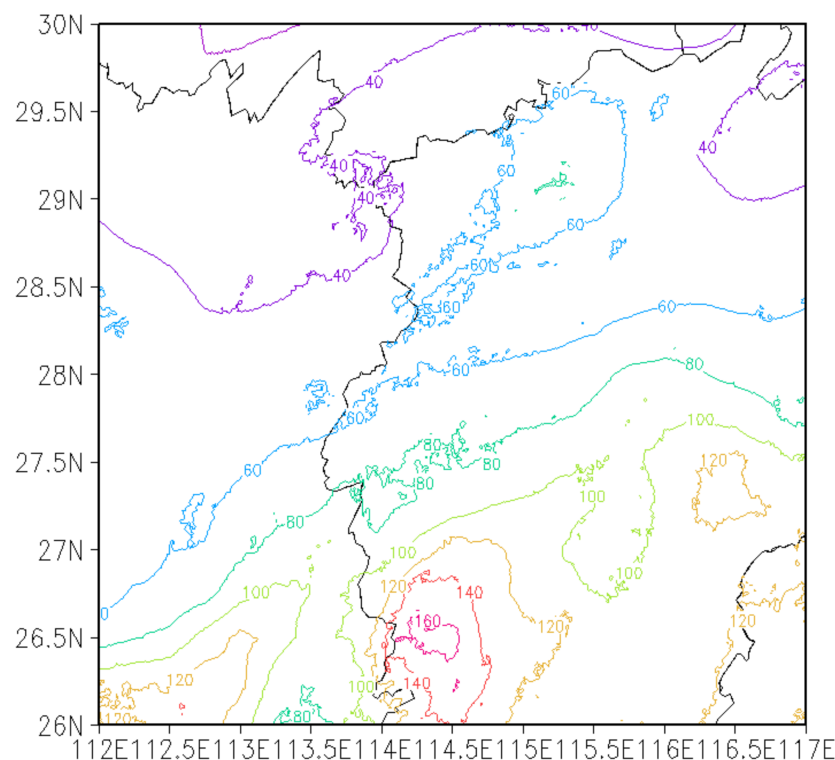


Figure 3. Average temperature (°C) of the coldest month, January, from 1961 to 2010.



**Figure 4.** Annual average precipitation (mm/per year) from 1961 to 2010.3. Climate change forecasts.

The RegCM model showed that in the future the annual average temperature and precipitation in the study area will experience an upward trend, the monthly average temperature will increase, and the continuous long-term warming trend will be significant, while the precipitation prediction showed characteristics of greater oscillation, frequency, and intensity, and a greater intra-year variation with no obvious inter-annual trend. Historical climate data from 1961 to 2010 show that there is a temperature increase of about  $0.13\text{ }^{\circ}\text{C}$  every 10 years and a precipitation increase of about  $43.5\text{ mm}$  every 10 years. The monthly average from 1961 to 2010 in the climate model data was set as the historical climate base line. Under the RCP4.5 emissions scenario, from 2010 to 2100, the temperature is predicted to increase by  $0.26\text{ }^{\circ}\text{C}$  and the precipitation to increase by  $49.1\text{ mm}$  every 10 years. Under the RCP8.5 emissions scenario, however, the temperature is predicted to increase by  $0.58\text{ }^{\circ}\text{C}$  and the precipitation to increase by  $70.1\text{ mm}$  every 10 years.

It can be seen that under both the RCP4.5 and RCP8.5 emissions scenarios, the average temperature is predicted to increase compared with the base line annual average, and this suggests that the temperature will continue to increase over the next 100 years. The future predicted inter-annual variation of precipitation is not clear however, for although the precipitation will increase year by year, the rate of increase is significantly lower than that from 1961 to 2010. The temperature is also predicted to rise rapidly.

#### 4. Analysis Tree Vertical Growth Trend under Climate Change

The climatic factor has become an important environmental factor affecting the success or failure of forest tree species [28]. In other words, the response of a forest to climate change is based on the response of individual plant species to climate change. In the next 100 years, under RCP4.5, the temperature in the study area is predicted to rise by  $1.3$  to  $2.3\text{ }^{\circ}\text{C}$ , and the predicted variation range of precipitation is estimated to be from between  $-10$  to  $+20\%$ , based on historical climate data. Climate change mainly changes the composition and structure of forest ecosystems through temperature, water, and change in sunshine and light intensity [29]. There is a general consensus that temperature and precipitation have a decisive impact on tree species diversity [30,31], where some tree

species withdraw from the original forest ecosystem, while some new species invade the original system, thus changing its composition and tree species diversity [32].

Over longer periods, climate change has a significant impact on most plants [33], and species migration, invasion and even extinction have a direct impact on forest ecological functions due to the disruption of the balance of biodiversity [34]. Climate change does not significantly change the dominance of forest-dominant species and subdominant species; however, the spatial distribution of tree species diversity does show changes within different time scales and different emission concentrations, especially under the influence of special terrains and topographies.

#### 4.1. Data Processing Method

An analysis of climate variables and principal component analysis needs to be undertaken to reduce the quantity of data involved in the calculation. Before the principal component analysis of climate factors, it was necessary to judge the number of principal components and process them with the “psych function” package in R software. A parallel analysis was undertaken to determine the magnitude of the Eigen values for the actual, simulated and resampled data, and the results are plotted, as shown in Figure 5.

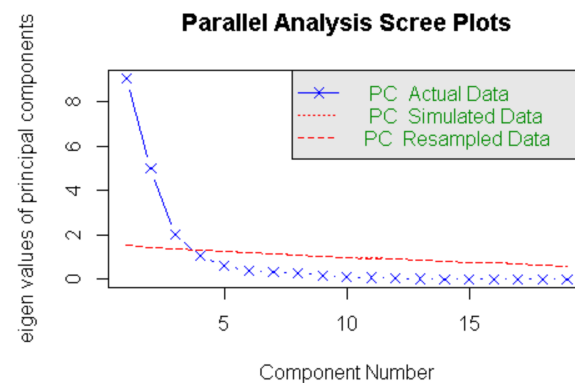


**Figure 5.** Gravel map of principal component analysis.

It can be seen from the gravel map of climates that there are three components above the red line, which suggests that climate factors can be reduced to these three principal components [35]. The “psych function” package was then used to obtain the weight of climate factors within the three principal components weight, shown as Table 1.

**Table 1.** Weight table of climatic factors in three principal components.

CFC	PC			RCP2.6			RCP4.5			RCP8.5		
	PC1	PC2	PC3	PC1	PC2	PC3	PC1	PC2	PC3	PC1	PC2	PC3
MAT	0.95	0.17	0.2	0.86	0.37	0.24	0.94	0.13	0.22	0.097	0.11	0.09
MWMT	0.48	0.76	0.11	0.24	0.81	0.24	0.58	0.63	0.27	0.81	0.44	0.21
MCMT	0.71	−0.44	−0.49	0.87	−0.36	−0.06	0.86	−0.39	−0.06	0.81	−0.44	−0.19
MAP	0.15	−0.79	0.47	−0.07	−0.64	0.71	−0.31	−0.44	0.8	0.13	−0.43	0.86
DD < 0	−0.83	0.41	0.26	−0.75	0.34	0.19	−0.79	0.41	0.13	−0.27	0.55	0.17
DD > 5	−0.91	0.26	0.28	0.75	0.5	0.29	0.91	0.2	0.25	0.97	0.14	0.11
PAS	−0.77	0.24	0.22	−0.81	0.34	0.27	−0.72	0.46	0.26	−0.59	0.59	0.26

MAT: Annual average temperature; MWMT: average hottest month temperature; MCMT: average coldest month temperature; MAP: annual average precipitation; DD < 0: days below 0 °C; DD > 5: days above 5 °C; PAS: precipitation from August of last year to July of this year; PC: principal components of base line; RCP2.6: principal components of RCP2.6; RCP4.5: principal components of RCP4.6; RCP8.5: principal components of RCP8.5.

The weight tables for climate factors contain too many intermediate values, and the distribution of most of the weights are not bipolar. An orthogonal rotation of the maximum variance of the data is therefore needed to make the weight distribution more

reasonable [36]. After orthogonal rotation, the correlation between climate factors and the three principal components (RC1, RC2, and RC3) were derived. The weight distribution effect of the principal components and climate factors was preliminarily checked and the orthogonal rotation, represented by a double plot, as shown Figure 6.

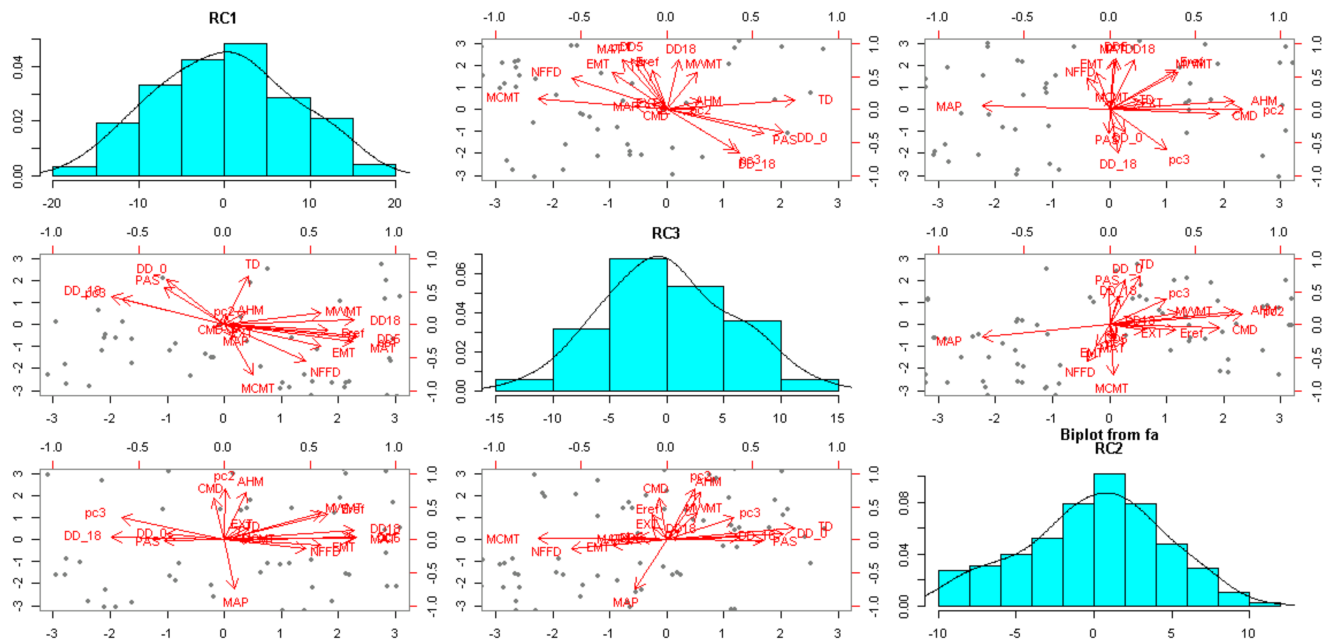


Figure 6. Orthogonal rotation of three principal components.

Rotation is a series of mathematical procedures intended to make the component load matrix easier to interpret. It denotes the components as much as possible, such that each component is explained only by a limited set of variables [37]. Orthogonal rotation with the maximum variance, the weights of the principal components and climate factors are optimized, and the obtained principal components are more reasonable. In order to establish the correlation between principal components and climate factors, it was then necessary to establish the correlation between climate factors and the three principal components, as shown Figure 7.

Only those correlations with the greatest relevance (>0.7) are expressed in Figure 7, where the significance of principal components and climate factors indicated by red lines is negative, and those indicated by black lines is positive. Similar processing was carried out for RCP2.6, RCP4.5 and RCP8.5 climate change data.

In order to judge that the three principal components of climate data are reasonable, it was necessary to calculate the cumulative variance of climate data after principal component analysis. Principal component variance is shown in Table 2.

Table 2. Principal components of climate variance.

ANOVA Categories	VPCPC		
	RC1	RC2	RC3
SS loadings	7.28	4.61	4.13
Proportion variance	0.38	0.24	0.22
Cumulative variance	0.38	0.63	0.84
Cumulative Proportion	0.45	0.74	1.00

ANOVA Categories: variance type; VPCPC: variance of climate principal components; SS loadings: sum of squares of columns of matrix; Proportion variance: variance ratio; Cumulative variance: cumulative variance; Cumulative Proportion: cumulative proportion.

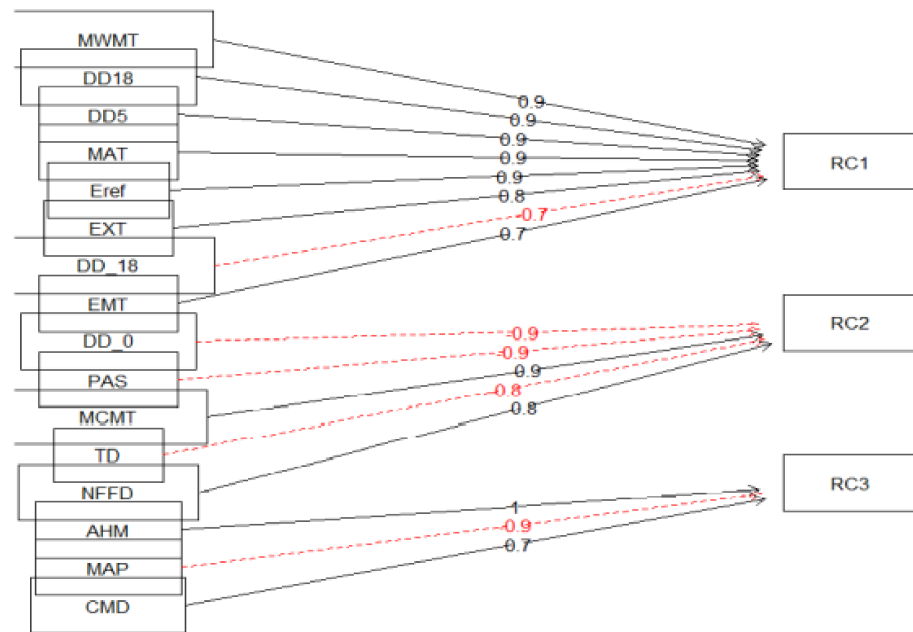


**Figure 7.** Correlation analysis between climatic factors and principal components.

It can be seen from Table 2 that the cumulative variance of climate data is about 80%, which shows that it was reasonable to use the three principal components in the above principal component analysis. The variance proportion was largest in the first principal component.

#### 4.2. Tree Vertical Theoretical Growth Equation

The height of trees is the most basic tree measurement factor in forest investigation, which is of great significance to the investigation of forest resources and forestry scientific research. Trees usually grow faster when there are sufficient resources, less environmental pressure and when they are in an advantageous position for light competition. The growth and distribution of the height of appropriate trees can therefore be used as an important basis for assessment of forest management activities and the prediction of stand growth and harvest outcomes. The height of trees is also widely used in forestry production assessment and prediction practice [38] and is a sensitive variable that can be used to characterize the possible impact of climate change on tree species succession [39].

The theoretical growth equation presently used in the research field of growth modeling includes the Mitscherlich equation [40], Richards equation [41], Korf equation [42] and the logistic function [43]. The logistic function is the most classic and commonly used in biological systems simulations [44] because the curve produced by the logistic model is versatile and can be adopted to simulate the rate of growth of a wide range of organisms and plants [45,46], and was therefore selected as the basic model in this study, as shown in Equation (1), where A represents the maximum parameter of tree growth, b represents the initial value, and c the maximum growth rate.

$$Y = \frac{A}{1 + be^{(-ct)}} \quad (1)$$

Determination of parameters is an important step for building a hybrid model, for it is necessary to clarify and define the fixed parameters and hybrid parameters. AIC (Akaike's Information Criterion) is based on maximum likelihood estimation and is still widely used to select an optimal prediction model from among several candidate models [47], and BIC (Bayesian Information Criterion) is one of the most popular criteria for model selection, which was derived under the assumption of independent and identical distribution. The choice of the best model is crucial in modeling data, and the criteria used in model selection

are therefore of critical importance. These criteria are based upon concepts of information and entropy, and focusing on a statistical approach provides a standard against which to weigh the complexity of the model and the goodness of fit of the data. The advantages and disadvantages are judged by the values of AIC, BIC and LL, through comparing AIC, BIC and the log likelihood (LL), the fewer the values, the better the values of AIC and BIC are, and the greater the LL is, meaning the better the model is [48].

The Logistic equation was used as the basic model, and climate factors were then added to model the tree vertical growth trend. In this paper, only tree height was used, as the simulation target for modeling assumed that the extinction of tree species is predicted from both changes in height of tree and crown width [49]. As shown in Equation (2), PPC1, PPC2 and PPC3 represent the three principal components of historical climate; A0, A1, A2, A3, B0, B1, B2, B3, C0, C1, C2 and C3 are fitting parameters that are based on Equation (1), which are fit by 1stOpt software package, and which are described in Section 4.3.  $Y_H$  represents height of tree.

$$Y_H = \frac{a0 + a1 \times ppc1 + a2 \times ppc2 + a3 \times ppc3}{1 + (b0 + b1 \times ppc1 + b2 \times ppc2 + b3 \times ppc3)e^{-(c0+c1 \times ppc1+c2 \times ppc2+c3 \times ppc3) \times t}} \tag{2}$$

### 4.3. Theoretical Equation Parameter Solution and Verification

In the field of nonlinear regression, commonly used software toolkits include MATLAB [50], SAS [51], SPSS [52], etc. All software toolkits need to provide appropriate initial parameter values, such that the calculation can converge and find the optimal solution; however, if the initial values of the parameters are inaccurate or set incorrectly, the calculation is difficult to converge, and an accurate result cannot be obtained. In practical applications, especially when there are many parameters, it is difficult to obtain appropriate initial values. In this paper, the 1stOpt software package was chosen, due to its strong optimization and fault tolerance [53]. In most cases, the correct results can be obtained from any random initial value [54]. In the present study, the parameters A0, A1, A2, A3, B0, B1, B2, B3, C0, C1, C2, C3 of the fitting equation were solved by 1stOpt, the algorithm was set as "BFGS + UGO", and parameter values generated by calculation were substituted into R software for nonlinear fitting verification, and the output results are shown in Table 3.

**Table 3.** Estimation fitting parameters of tree vertical growth model.

Variable	Parameter	Asymptotic Estimate	RSS	T Value	p Value	SE	Sig
$Y_H$	a0	−3.315+01	397.5	−3.044	0.00261	1.0894+1	**
	a1	1.739e-02		4.649	5.64e-06	3.740e-03	***
	a2	−1.599e-02		−4.758	3.47e-06	3.362e-03	***
	a3	4.584e-02		4.847	2.31e-06	9.457e-03	***
	b0	−3.019e+01		−1.633	0.10387	1.849e+01	
	b1	8.882e-03		1.430	0.15422	6.213e-03	
	b2	−4.078e-03		−0.815	0.41445	5.003e-03	
	b3	8.146e-03		0.563	0.57410	1.446e-02	
	c0	4.547e-01		2.748	0.00064	1.654e-01	**
	c1	−1.633e-04		−2.801	0.00554	5.830e-05	**
	c2	1.718e-04		2.741	0.00662	6.268e-05	**
	c3	−5.305e-04		−3.339	0.00098	1.589e-04	***

Sig: significance; Signif. codes: '\*\*\*' 0.001, '\*\*' 0.01, '\*' 0.05; RSS: sum of squares of residuals; SE: standard error; T value and p value are used to judge whether they are statistically significant or not.

The table shows that the fitting results of all parameters were significant ( $p < 0.05$ ), except for B0, B1, B2 and B3 ( $p > 0.05$ ). The random effect of those parameters not meeting the level of significance were deemed to not contribute to the whole model in this simulation and were therefore eliminated. After eliminating the insignificant fitting parameters, the remaining fitting parameters are shown in Table 4.

**Table 4.** Tree vertical growth model fitting results.

Parameter	Asymptotic Estimate	RSS	SE	T Value	p Value	Sig
a0	−3.09e+01		1.11E01	−2.779	0.0059	**
a1	1.66E-02		3.79E-03	4.377	1.83e-05	***
a2	−1.62e-02		3.56e-03	−4.549	8.73e-06	***
a3	4.45e-02		9.61e-03	4.632	6.06e-06	***
b0	−1.77e+01		8.94e+01	−1.943	0.048418	*
b1	5.09e-03	0.2325	1.97e-03	2.589	0.010313	*
b2	4.09e-02		0.97e-01	4.589	0.213313	*
b3	−0.03e-01		7.67e-01	−1.463	0.513215	*
c0	5.09e-01		1.51e-01	3.371	0.000878	***
c1	−1.78e-04		5.03e-05	−3.536	0.000491	***
c2	2.04e-04		5.43e-05	3.74	0.000223	***
c3	−5.68e-04		1.34e-04	−4.239	3.25e-05	***

Sig: significance; Signif. codes: '\*\*\*' 0.001, '\*\*' 0.01, '\*' 0.05; RSS: sum of squares of residuals; SE: standard error; Sig: significance; T value and p value are used to judge whether they are statistically significant or not.

All parameters are significant ( $p < 0.05$ ) and therefore meet the requirements that the p value is less than 0.05, and the calculation results of these fitting parameters of the tree vertical growth model were used to establish NLME model.

#### 4.4. Optimal Nonlinear Mixed Effects Growth Model

The analytical data of *Cyclobalanopsis glauca* and analytic data in plots 1–3 were fitted by the Optimal NLME tree vertical growth model, and the full combination of the random effect parameters was generated by using the Python software (Version 3.7.1). NLME function package was used to fit the nonlinear mixing effect. The best tree vertical growth model was then selected on the basis of AIC, BIC and LL, as shown in Table 5.

**Table 5.** Comparison parameters of tree vertical growth nonlinear mixed effect model.

NO.	AIC	BIC	LL
H8	626.0595	667.8247	−302.0297
H19	602.993	644.7607	−289.4965
H34	587.8403	636.5692	−279.9201
H123	605.8847	654.6172	−288.9442
H187	591.7608	650.9854	−270.8873
H190	568.8145	627.9854	−267.4073

AIC, Akaike Information Criterion; BIC, Bayesian information criterion; LL, log likelihood.

It can be deduced from Table 5 that the AIC and BIC values of the model labeled NO.H190 are relatively small, and the LL value is the largest. Through comprehensive comparison, it was concluded that the NO.H190 was the optimal nonlinear mixed effect growth model for tree vertical data in this sample plot. Using the obtained parameters, the random effect results of model NO.H190 nonlinear mixed effect fitting for B0, B1 and C3 are shown Table 6.

**Table 6.** Random effect fitting results.

Parameter	Standard Deviation	Correlation Coefficient
b0	6.589829e+00	b0
b1	1.252336e-03	−0.949
b3	2.323323e-05	0.311
		b1
		−0.593

The fixed effect results of model NO.H190 NLME fitting for B0, B1 and C3 are shown in Table 7.

**Table 7.** Fixed effect fitting result.

Parameter	Value	Standard Deviation	T Value	p Value
a0	−16.270252	7.886	−2.063182	0.0403
a1	0.011659	0.002803	4.159749	0.0000
a2	−0.009873	0.002452	−4.026889	0.0001
a3	0.030090	0.007258	4.146001	0.0000
b0	14.508964	3.694393	3.927293	0.0001
b1	−0.001797	0.000763	−2.353443	0.0195
c0	0.424091	0.067631	6.270649	0.0000
c1	−0.000109	0.000023	−4.758027	0.0000
c2	0.000072	0.000021	3.402815	0.0008
c3	−0.000229	0.00059	−3.866325	0.0001

In Table 7, where all parameters are significant ( $p < 0.05$ ), the Equation NO.H190 was chosen as the optimal NLME of a tree vertical growth model. The optimal model of tree vertical growth can therefore be determined according to the values of the fitted parameters, as shown in Equation (3).

$$Y_H = \frac{-16.270252 + 0.011659X_1 - 0.009873X_2 + 0.030090X_3}{1 + (14.508964 - 0.001797X_1)e - (0.424091 - 0.000109x_1 + 0.000072x_2 - 0.0000299x_3)T} \quad (3)$$

$X_1$ ,  $x_2$  and  $x_3$ , as independent variables to be used as future climate factors, are described in Section 4.1.  $Y_H$  is the height of the tree of the Optimal NLME growth model, which is the determined model used in this paper.

#### 4.5. Model Fitting and Accuracy Assessment

Once the best fitting model had been selected, the climate principal component scores under the three climate scenarios could be substituted into the model to predict the growth trend of *Cyclobalanopsis glauca* until 2100. In this paper, the determination coefficient ( $R^2$ ), mean absolute deviation (MAB), mean relative error absolute value (RMA) and root mean square error (RMSE) were used to compare the model accuracy. In order to evaluate the accuracy of fitting of the tree vertical growth trend,  $R^2$ , MAB, RMA and RMSE of the analytical data and model fitting data were calculated, as shown in Table 8.

**Table 8.** Table of tree vertical growth model equation fitting accuracy.

NO.	RMSE	$R^2$	MAB	RMA
H8	0.7204364	0.963157	0.5497517	0.108974
H19	0.6826036	0.966924	0.5102679	0.104489
H34	0.6124327	0.973375	0.4659912	0.098020
H123	0.6808649	0.967093	0.5082457	0.104659
H187	0.6081427	0.973747	0.4632668	0.096757
H190	0.5433629	0.979042	0.4346239	0.094244

It can be seen from the accuracy of the fitting table that the  $R^2$  of equation No. H190 was closest to 1, and RMSE, MAB and RMA are the minimum values of the parameters [55], and it is obvious that this model is the best tree vertical growth model. When there is a random effect, the residual value fluctuates greatly, and after adding a random effect, the residual value was more densely distributed near 0, which represents a better effect, and can thus improve the accuracy of fitting and can be used to simulate the tree vertical growth trend under climate change.

#### 4.6. *Cyclobalanopsis glauca* Vertical Growth Trend Prediction

Using the optimal NLME growth model (equation of No.H190), and under the RCP2.6, RCP4.5 and RCP8.5 emissions scenarios, three climate principal components, which are the

main climatic elements as independent variables, can be used to model the *Cyclobalanopsis glauca* growth trend in the future, as shown in Figures 8–10.

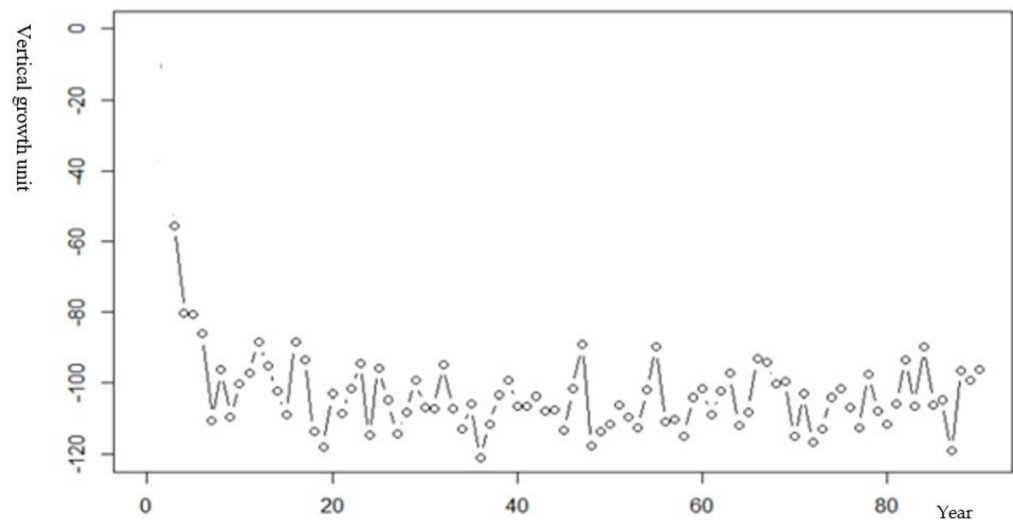


**Figure 8.** Growth of tree vertical under the RCP2.6 emissions scenario.

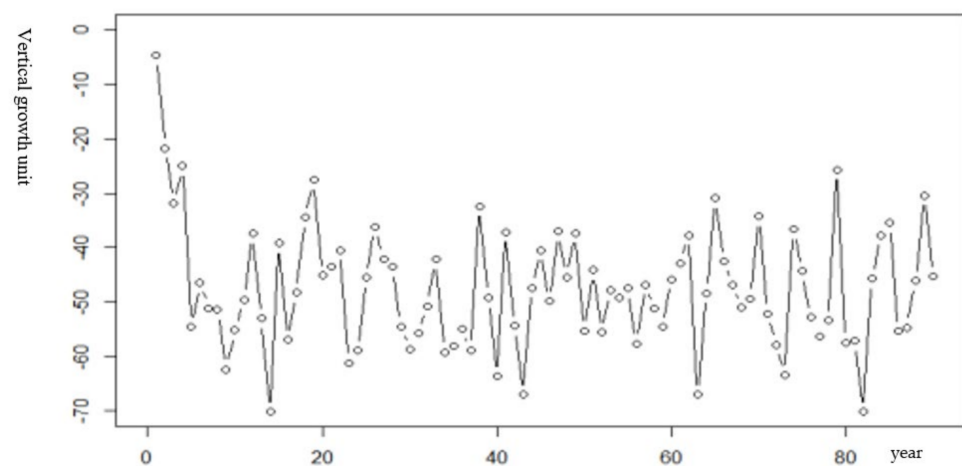


**Figure 9.** Growth of tree vertical under the RCP4.5 emissions scenario.

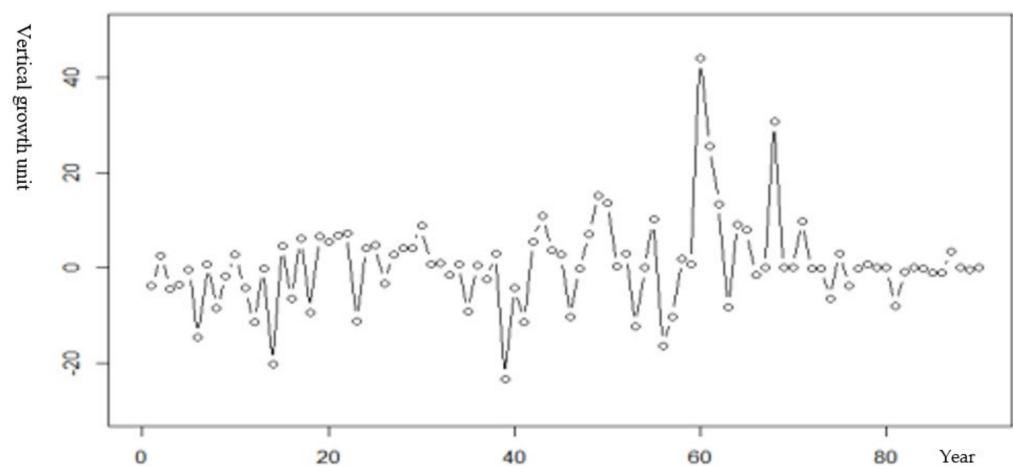


**Figure 10.** Growth of tree vertical under the RCP8.5 emissions scenario.

As can be seen from a comparison of Figures 8–10, under the emissions scenario of RCP2.6, there is an inhibitory effect on the vertical growth of *Cyclobalanopsis glauca*, which

is shown in Figure 8, where the predicted results are mostly distributed between  $-60$  and  $-120$  units. Under the emissions scenario of RCP4.5, there is also an inhibitory effect, with predicted results distributed between  $-30$  and  $-65$  units as shown in Figure 9. Under the RCP8.5 emissions scenario, however, the growth of *Cyclobalanopsis glauca* will be promoted, as reflected in the predicted results in Figure 10, which are mostly distributed between  $10$  and  $-20$  units.

## 5. Discussion

The aim of this paper was to simulate the vertical growth of *Cyclobalanopsis glauca* under climate change. The results show that the promotion and inhibition of vertical growth of *Cyclobalanopsis glauca* under three different climate change scenarios may occur at the same time, but to different degrees. The degree to which climate change will affect the tree species in the study area can be predicted and may change the distribution pattern of tree species diversity in the study area. The vertical growth prediction of *Cyclobalanopsis glauca* based on RegCM and NLME can better integrate the research results of world climate change and tree species growth model, especially in the dynamic downscaling application of RegCM to GCM. This is innovative in terms of both means and methods and shows how the dynamic application of climate change data can inform and improve the timeliness and scientific rigor of forestry management policy.

### 5.1. Trend of *Cyclobalanopsis glauca* Growth under Climate Change Scenarios

Climate change certainly impacts upon the migration and succession of tree species; however, there is still a great debate concerning the magnitude of the final impact under various climate change scenarios. The results show that the comprehensive effects of different climate change scenarios on tree vertical growth can either promote or inhibit the growth of specific climate-sensitive species. This simulation indicates that climate change will have an obvious effect on the overall growth of *Cyclobalanopsis glauca*. The growth inhibition effect is obvious under the RCP2.6 and RCP4.5 emissions scenarios, where the effect of the RCP4.5 scenario is predicted to inhibit tree vertical growth, although not as much as in the RCP2.6 emissions condition by the year 2100. Under the RCP8.5 emissions scenario, the growth promotion effect on the tree vertical growth will become obvious.

### 5.2. A Dynamic Implementation of an Integrated Model of Large-Scale Climate Data to Predict Micro Environmental Change

RegCM can better reflect the characteristics of climate change by providing higher resolution features than those obtained from global climate models. In this paper, the distribution of climatic elements is presented in high resolution by downscaling and by introducing detailed location-specific climatic conditions into the nonlinear mixed effect growth model, which greatly improved the simulation accuracy. This simulation indicates how *Cyclobalanopsis glauca* growth can be promoted, or inhibited, by localized regional climate change. In this article, only the data of RegCM are downscaled and substituted into the optimal NLME model, and the growth and extinction trend map of *Cyclobalanopsis glauca* cannot be generated, which is also the deficiency of this study. Different models have different algorithm complexity and data processing methods; thus, there are different degrees of deviation in the simulation, and as more and more accurate environmental data are obtained, it is expected that more and better models with more accurate predictions will be developed in the future.

### 5.3. Further Study

The influence of climate on trees is not only reflected in tree vertical height, but also on DBH (Diameter at Breast Height) and tree biomass. In future research, it is therefore necessary to simulate the impact of climate change on DBH, biomass and other properties of tree growth. It is expected that, as a result of this study of *Cyclobalanopsis glauca*, this simulation process can be extended to other tree species. Finally, by analyzing the extinction

of all other tree species in the study area, under various emission conditions, the tree species diversity can be reflected indirectly.

The climate changes ranging from suitable to unsuitable for *Cyclobalanopsis glauca*, or vice versa, are not the same as the disappearance or not of this species distribution in this area, as it may also be affected by environmental pressure. The significant environmental factors for species growth include light, soil, terrain, vegetation factors, and neighborhood competition between species. Although as many climate factors as possible were taken into consideration in this paper, and a principal component analysis was undertaken, there is still an insufficiency of other environmental variables considered in the model. The basic model is, however, worthy of optimization and in order to determine whether the model is worthy of further study, further simulations are necessary, taking into account additional environmental factors that may provide a better growth model suitable for simulating the response of *Cyclobalanopsis glauca* vertical growth to climate change in the study area, especially in local regional climatic conditions. In addition, in order to quantitatively analyze the response of a species under environmental stress, differences of species growth characteristics under different environmental conditions need be compared through multiple homogeneous experiments, combined with methylation and simplified genome or transcriptome sequencing to reveal the response trend of other species to climate change at the micro level.

#### 5.4. Study Limitations

The effects of climate on *Cyclobalanopsis glauca* oak are not absolutely the same under different emission conditions, which reflects the complex effects of regional climate, geographical location, topography and other factors affecting tree species diversity. Of course, this deviation may also be caused by using small sample plots, an insufficient number of plots or data samples, data measurement inaccuracy, or the imperfect data processing method, which may lead to the potential overall inaccuracy of the model, thus increasing the uncertainty of predictions, which are also the limitations of this study.

Uncertainty is a common phenomenon in the natural environment that cannot be completely avoided, nor the causes of uncertainty eliminated. We can however improve the accuracy of simulations by constantly improving the specificity and accuracy of the data, and of the processing methods, and by the addition of more environmental factors.

**Author Contributions:** Supervision, G.Z.; writing and review, H.D. All authors have read and agreed to the published version of the manuscript.

**Funding:** This research received funding from Science and Technology Innovation Platform and Talent Plan Project of Hunan Province under Grant 2017TP1022.

**Data Availability Statement:** The data presented in this study are available on request from the corresponding author. The data are not publicly available due to their relevance of an ongoing Ph.D. thesis.

**Acknowledgments:** We acknowledge the World Climate Research Program, which through its working group on coupled modeling, coordinated and promoted CMIP6. The authors would like to thank Li Jianjun and Sang Jie for assistance in material collection and data processing.

**Conflicts of Interest:** The authors declare no conflict of interest.

## References

1. Li, Q.X.; Sun, W.; Huang, B.; Dong, W. Consistency of global warming trends strengthened since 1880s. *Sci. Bull.* **2020**, *65*, 1709–1712. [[CrossRef](#)]
2. Korell, L.; Auge, H.; Chase, J.M.; Harpole, S.; Knight, T.M. We need more realistic climate change experiments for understanding ecosystems of the future. *Glob. Change Biol.* **2020**, *26*, 325–327. [[CrossRef](#)] [[PubMed](#)]
3. He, X.Y.; Liang, J.; Zeng, G.; Yuan, Y.; Li, X. The Effects of Interaction between Climate Change and Land-Use/Cover Change on Biodiversity-Related Eco system Services. *Glob. Chall.* **2019**, *3*, 1800095. [[CrossRef](#)] [[PubMed](#)]
4. Wielgoss, A.; Tschamtker, T.; Buchori, D.; Fiala, B.; Clough, Y. Temperature and a dominant dolichoderine ant species affect ant diversity in Indonesian cacao plantations. *Agric. Ecosyst. Environ.* **2010**, *135*, 253–259. [[CrossRef](#)]

5. Cailleret, M.; Jansen, S.; Robert, E.M.R.; Desoto, L.; Aakala, T.; Antos, J.A.; Beikircher, B.; Bigler, C.; Bugmann, H.; Caccianiga, M.; et al. A synthesis of radial growth patterns preceding tree mortality. *Glob. Change Biol.* **2017**, *23*, 1675–1690. [[CrossRef](#)]
6. Chen, X.W.; Li, B.L. Tree diversity change in remaining primary mixed-broadleaved Korean pine forest under climate change and human activities. *Biodivers. Conserv.* **2004**, *13*, 563–577. [[CrossRef](#)]
7. Chen, M.X.; Yue, X.; Pengling, W.; Zijin, D. Climate change and multi-dimensional sustainable urbanization. *J. Geogr. Sci.* **2021**, *31*, 1328–1348. [[CrossRef](#)]
8. Shen, Q.N.; Cong, Z.T.; Lei, H.M. Evaluating the impact of climate and underlying surface change on runoff within the Budyko framework: A study across 224 catchments in China. *J. Hydrol.* **2017**, *554*, 251–262. [[CrossRef](#)]
9. Ma, J.-J.; Yao, H.; Feng, Z.-Y.; Zhang, S.-L. Changes in plant functional groups and species diversity under three grassland using modes in typical grassland area of Inner Mongolia, China. *Chin. J. Plant Ecol.* **2012**, *36*, 1–9. [[CrossRef](#)]
10. Hu, H.-Q.; Liu, H.-L.; He, J.-Z.; Huang, Q.-Y. Effect of selected organic acids on cadmium sorption by variable- and permanent-charge soils. *Pedosphere* **2007**, *17*, 117–123. [[CrossRef](#)]
11. Li, W.-J.; Hu, J.; Feng, T.; Qing, L. Dynamics of Potential Distribution of Cyclobalanopsis Forest in Guizhou Province of China under Global Climate Change. *J. Trop. Subtrop. Bot.* **2020**, *28*, 145–152. [[CrossRef](#)]
12. Zhou, S.X.; Yu, H.B. Comparison and analysis of tree height calculation methods for tree trunk analysis of different age rs. *For. Inventory Plan.* **1989**, *4*, 21–27. (In Chinese)
13. Carvalho, D.; Rocha, A.; Costoya, X.; deCastro, M.; Gómez-Gesteira, M. Wind energy resource over Europe under CMIP6 future climate projections: What changes from CMIP5 to CMIP. *Renew. Sustain. Energy Rev.* **2021**, *151*, 111594. [[CrossRef](#)]
14. Zamani, Y.; Monfared, H.; Arman, S.; Mehdi, A.M.; Mohsen, H. A comparison of CMIP6 and CMIP5 projections for precipitation to observational data: The case of Northeast Iran. *Theor. Appl. Climatol.* **2020**, *142*, 1613–1623. [[CrossRef](#)]
15. Chen, S.N.; Guo, J. Spatial interpolation techniques: Their applications in regionalizing climate-change series and associated accuracy evaluation in Northeast China. *Geomat. Nat. Hazards Risk* **2017**, *8*, 689–705. [[CrossRef](#)]
16. Duan, H.L.; Cao, F.X. Numerical Simulation of Regional climate models in a Subtropical Region of China. In Proceedings of the 3rd International Conference on Environmental Science and Information Application Technology (ESIAT), Changsha, China, 20–21 August 2011. [[CrossRef](#)]
17. Wang, X.Q.; Huang, G.H.; Liu, J.L. Projected increases in near-surface air temperature over Ontario, Canada: A regional climate modeling approach. *Clim. Dyn.* **2015**, *45*, 1381–1393. [[CrossRef](#)]
18. Xin, X.G.; Wu, T.; Zhang, J.; Yao, J.; Fang, Y. Comparison of CMIP6 and CMIP5 simulations of precipitation in China and the East Asian summer monsoon. *Int. J. Climatol.* **2020**, *40*, 6423–6440. [[CrossRef](#)]
19. Xu, Z.; Han, Y.; Tam, C.Y.; Yang, Z.-L.; Fu, C. Bias-corrected CMIP6 global dataset for dynamical downscaling of the historical and future climate (1979–2100). *Sci. Data* **2021**, *8*, 293. [[CrossRef](#)]
20. Gutowski, W.J. The ongoing need for high-resolution regional climate models: Process understanding and stakeholder information. *Bull. Am. Meteorol. Soc.* **2020**, *101*, 664–683. [[CrossRef](#)]
21. Sun, F.; Walton, D.; Hall, A. A Hybrid Dynamical-Statistical Downscaling Technique, Part II: End-of-Century Warming Projections Predict a New Climate State in the Los Angeles Region. *J. Clim.* **2015**, *28*, 4618–4636. [[CrossRef](#)]
22. Maharana, P.; Dimri, A.P. Impact of initial and boundary conditions on regional winter climate over the Western Himalayas: A fixed domain size experiment. *Glob. Planet. Change* **2014**, *114*, 1–13. [[CrossRef](#)]
23. Jiang, D.; Tian, Z.; Lang, X. Reliability of climate models for China through the IPCC Third to Fifth Assessment Reports. *Int. J. Climatol.* **2016**, *36*, 1114–1133. [[CrossRef](#)]
24. Gao, X.J.; Giorgi, F. Use of the RegCM System over East Asia: Review and perspectives. *Engineering* **2017**, *3*, 766772. [[CrossRef](#)]
25. Song, T.Y.; Huang, G.; Li, Y.; Wang, X.; Lu, C.; Shen, Z. Bayesian model averaging of the RegCM temperature projections: A Canadian case study. *J. Water Clim. Change* **2022**, *13*, 771–785. [[CrossRef](#)]
26. Harris, I.; Osborn, T.J.; Jones, P.; Lister, D. Version 4 of the CRU TS monthly high-resolution gridded multivariate climate dataset. *Sci. Data* **2020**, *7*, 109. [[CrossRef](#)]
27. Schumann, G.J.P.; Bates, P.D. The Need for a High-Accuracy, Open-Access Global DEM. *Front. Earth Sci.* **2018**, *6*, 225. [[CrossRef](#)]
28. Zhang, L.J.; Zhu, L.; Li, Y.; Zhu, W.; Chen, Y. Maxent Modelling Predicts a Shift in Suitable Habitats of a Subtropical Evergreen Tree (*Cyclobalanopsis glauca* (Thunberg) Oersted) under Climate Change Scenarios in China. *Forests* **2022**, *13*, 126. [[CrossRef](#)]
29. Chen, G.Y.; IOP. Analysis on the Influence of the Climate Changes on the Global Vegetation. In Proceedings of the 6th International Conference on Advances in Energy, Environment and Chemical Engineering (AEECE), Electronic Network, Shanghai, China, 19–21 June 2020. [[CrossRef](#)]
30. Marty, C.; Duchesne, L.; Couture, S.; Gagnon, C.; Houle, D. Effects of climate and atmospheric deposition on a boreal lake chemistry: A synthesis of 36 years of monitoring data. *Sci. Total Environ.* **2021**, *758*, 143639. [[CrossRef](#)]
31. Gu, Y.; Han, S.; Zhang, J.; Chen, Z.; Wang, W.; Feng, Y.; Jiang, Y.; Gen, S. Temperature-Dominated Driving Mechanisms of the Plant Diversity in Temperate Forests, Northeast China. *Forests* **2020**, *11*, 227. [[CrossRef](#)]
32. Wang, T.; Wang, G.; Innes, J.; Nitschke, C.; Kang, H. Climatic niche models and their consensus projections for future climates for four major forest tree species in the Asia-Pacific region. *For. Ecol. Manag.* **2016**, *360*, 357–366. [[CrossRef](#)]
33. Peng, J.-Q.; Cao, F.-X.; Liu, Z.; Li, M.; Duan, H.-L.; Xiong, Y.-L.; Lü, C.; Luo, X.F. Effect of climate factors on *Mytilaria laosensis* population and distribution forecasting in the future. *Sheng Taixue Zazhi* **2014**, *33*, 1150–1156.

34. Zhou, H.; Luo, Y.; Zhou, G.; Yu, J.; Shah, S.; Meng, S.; Liu, Q. Exploring the Sensitivity of Subtropical Stand Aboveground Productivity to Local and Regional Climate Signals in South China. *Forests* **2019**, *10*, 71. [[CrossRef](#)]
35. King, J.R.; Jackson, D.A. Variable selection in large environmental data sets using principal components analysis. *Environmetrics* **1999**, *10*, 67–77. [[CrossRef](#)]
36. Wang, W.S.; Tang, Y. Watershed Flood Forecasting Based on Cluster Analysis and BP Neural Network. In Proceedings of the 13th CCF Conference on Computer Supported Cooperative Work and Social Computing, Guilin, China, 30 October 2020. [[CrossRef](#)]
37. Evans, P.R. Rotations and rotation matrices. *Acta Crystallogr. Sect. D-Biol. Crystallogr.* **2001**, *57*, 1355–1359. [[CrossRef](#)] [[PubMed](#)]
38. Andales, A.; Wang, J.; Sammis, T.W.; Mexal, J.G.; Simmons, L.J.; Miller, D.R.; Gutschick, V.P. A model of pecan tree growth for the management of pruning and irrigation. *Agric. Water Manag.* **2006**, *84*, 177–188. [[CrossRef](#)]
39. O'Neill, G.A.; Nigh, G. Linking population genetics and tree height growth models to predict impacts of climate change on forest production. *Glob. Change Biol.* **2011**, *17*, 3208–3217. [[CrossRef](#)]
40. Prasad, S. An algebraic model from mitscherlich function to describe lactation curves of dairy animals. *J. Appl. Anim. Res.* **2007**, *31*, 121–123. [[CrossRef](#)]
41. Florica, A.; Pop, I.; Micula, M. Features of the Bertalanffy-Richards growth model in forestry. In Proceedings of the Symposium on Prospects for the 3rd Millenium Agriculture, Cluj Napoca, Romania, 5–6 October 2006.
42. Nafidi, A.; El Azri, A. A stochastic diffusion process based on the Lundqvist-Korf growth: Computational aspects and simulation. *Math. Comput. Simul.* **2021**, *182*, 25–38. [[CrossRef](#)]
43. Dominguez-Almendros, S.; Benitez-Parejo, N.; Gonzalez-Ramirez, A.R. Logistic regression models. *Allergol. Immunopathol.* **2011**, *39*, 295–305. [[CrossRef](#)]
44. Acevedo, M.A.; Marcano, M.; Fletcher, R.J. A diffusive logistic growth model to describe forest recovery. *Ecol. Model.* **2012**, *244*, 13–19. [[CrossRef](#)]
45. Kilian, H.G.; Bartkowiak, D.; Kazda, M.; Kaufmann, D. Modelling the growth of plants with a uniform growth logistics. *J. Theor. Biol.* **2014**, *349*, 57–65. [[CrossRef](#)] [[PubMed](#)]
46. Kawano, T.; Wallbridge, N.; Plummer, C. Logistic Models for Simulating the Growth of Plants by Defining the Maximum Plant Size as the Limit of Information Flow. *Plant Signal. Behav.* **2020**, *15*, 1709718. [[CrossRef](#)] [[PubMed](#)]
47. Song, E.; Won, S.; Lee, W. Using the corrected Akaike's information criterion for model selection. *Korean J. Appl. Stat.* **2017**, *30*, 119–133. [[CrossRef](#)]
48. Gomez, E.V.; Schaalje, G.B.; Fellingham, G.W. Performance of the Kenward-Roger method when the covariance structure is selected using AIC and BIC. *Commun. Stat. Simul. Comput.* **2005**, *34*, 377–392. [[CrossRef](#)]
49. Forrester, D.I.; Benneter, A.; Bouriaud, O.; Bauhus, J. Diversity and competition influence tree allometric relationships—Developing functions for mixed-species forests. *J. Ecol.* **2017**, *105*, 761–774. [[CrossRef](#)]
50. Ehinger, B.V.; Dimigen, O. Unfold: An integrated toolbox for overlap correction, non-linear modeling, and regression-based EEG analysis. *PeerJ* **2019**, *7*, 7838. [[CrossRef](#)] [[PubMed](#)]
51. Li, L.-L.; Li, F.-R.; Jia, W.-W.; Dong, L.-H. Prediction Model of Nut Yields for Korean Pine Plantation. *Bull. Bot. Res.* **2014**, *34*, 349–355. [[CrossRef](#)]
52. Kim, W.-J.; Kim, K.-S.; Jeong-II, L.; Lee, H. Linear, Non-Linear and Time Series Model Verification for Forecasting the Change of Grade Increase Applicants -Focusing on Gyeonggi Region. *Taekwondo J. Kukkiwon* **2017**, *8*, 169–190. [[CrossRef](#)]
53. Cheng, X.Y.; Long, W.F.; Liu, H.L.; Yang, S.M. The Global Optimization Package 1stOpt and its Application in Engineering Hydrology. In Proceedings of the 4th International Yellow River Forum, Yellow River Conservancy Commission, Zhengzhou, China, 20–23 October 2009.
54. He, Z.L.; Yu, H.X. Data Fusion Based on First Optimization and Its Comparison with the Traditional Algorithms. In Proceedings of the 6th International Congress on Image and Signal Processing (CISP), Hangzhou, China, 16–18 December 2013.
55. Chai, T.; Draxler, R.R. Root mean square error (RMSE) or mean absolute error (MAE)?—Arguments against avoiding RMSE in the literature. *Geosci. Model Dev.* **2014**, *7*, 1247–1250. [[CrossRef](#)]